HHS Public Access

Author manuscript

Cell Rep. Author manuscript; available in PMC 2019 January 02.

Published in final edited form as:

Cell Rep. 2018 June 19; 23(12): 3525–3536. doi:10.1016/j.celrep.2018.05.072.

Salmonella activation of STAT3 signaling by SarA effector promotes intracellular replication and production of IL-10

Sarah L. Jaslow[1], **Kyle D. Gibbs**[1], **W. Florian Fricke**[2], **Liuyang Wang**[1], **Kelly J. Pittman**[1], **Mark K. Mammel**[3], **Joshua T. Thaden**[4], **Vance G. Fowler Jr.**[4], **Gianna E. Hammer**[5], **Johanna R. Elfenbein**[6], and **Dennis C. Ko**[1,4,7]

[1]Department of Molecular Genetics and Microbiology, School of Medicine, Duke University, Durham, NC 27710

[2]Department of Nutrigenomics, University of Hohenheim, Stuttgart, Germany

[3]Division of Molecular Biology, Center for Food Safety and Applied Nutrition, U.S. Food and Drug Administration, Laurel, MD 20708

[4]Division of Infectious Diseases, Department of Medicine, School of Medicine, Duke University, Durham, NC 27710

[5]Department of Immunology, School of Medicine, Duke University, Durham, NC 27710

[6]Department of Clinical Sciences, College of Veterinary Medicine, North Carolina State University, Raleigh, NC 27607

[7]Lead Contact

Summary

Salmonella enterica is an important foodborne pathogen that utilizes secreted effector proteins to manipulate host pathways to facilitate survival and dissemination. Different *S. enterica* serovars cause disease syndromes ranging from gastroenteritis to typhoid fever and vary in their effector repertoire. We leveraged this natural diversity to identify *stm2585*, here designated *sarA* (*Salmonella anti-inflammatory response activator*), as a *Salmonella* effector that induces production of the anti-inflammatory cytokine IL-10. RNA-seq of cells infected with either Δ*sarA* or wild-type *S.* Typhimurium revealed that SarA activated STAT3 transcriptional targets. Consistent with this, SarA was necessary and sufficient for STAT3 phosphorylation, STAT3 inhibition blocked IL-10 production, and SarA and STAT3 interacted by co-immunoprecipitation. These effects of SarA contributed to intracellular replication *in vitro* and bacterial load at systemic sites in mice. Our results demonstrate the power of using comparative genomics for identifying

*To whom correspondence should be addressed: dennis.ko@duke.edu.

Author Contributions:

SLJ, KDG, and DCK wrote the manuscript. All authors critically reviewed manuscript revisions and contributed intellectual input to the final submission. SLJ, KDG, and DCK planned and carried out experiments and analysis. WFF and LW carried out analysis and visualization of comparative genomics. KJP assisted with mouse intraperitoneal experiments. JRE provided intellectual contributions and carried out mouse oral infection experiments. MKM, JTT, VGF, and GEH provided biological samples, mice, and intellectual input.

Accession Numbers: RNA-seq data are available in GEO (GSE104354).

Declaration of Interests: The authors declare no competing interests.

effectors and that *Salmonella* has evolved mechanisms for activating an important anti-inflammatory pathway.

Keywords

Salmonella; STAT3; B cell; salmonella pathogenicity island-2; IL-10; comparative genomics; RNAseq; gifsy phage; anti-inflammatory; evolution

Introduction

Non-typhoidal salmonellosis, caused by *Salmonella enterica* serovars such as Typhimurium and Enteritidis, is a major foodborne illness and a leading cause of gastroenteritis. The World Health Organization estimates that non-typhoidal *Salmonella* infections caused 150 million cases of gastroenteritis and 600,000 cases of bacteremia in 2010, which resulted in the global loss of 8.3 million disability adjusted life years, the highest burden of any foodborne illness (Kirk et al., 2015; Majowicz et al., 2010).

Salmonellae have evolved an impressive repertoire of secreted effectors that manipulate the host. These effectors, translocated into the host cell through two type-three secretion systems (T3SS) encoded in *Salmonella* pathogenicity islands (SPI-1 and SPI-2), hijack host cell physiology, enable invasion, and help establish an intracellular niche inside a *Salmonella*-containing vacuole (SCV) (Jennings et al., 2017; Moest and Méresse, 2013). Critically important in establishing infection, *Salmonella* T3SSs activate pro-inflammatory pathways to overcome colonization resistance in the gut (Keestra et al., 2011; Stecher et al., 2007; Winter et al., 2010).

Salmonella also suppresses inflammation, but these activities are less well understood. *Salmonella* effectors, such as SspH1, AvrA, and GogB, suppress NFκB signaling (Collier-Hyams et al., 2002; Haraga and Miller, 2003; Pilar et al., 2012). GogB interacts with Skp1 and FBX022 to inhibit IκB degradation and thus NFκB activation (Pilar et al., 2012). Immune recognition of *Salmonella* can also trigger a key mediator of anti-inflammatory responses, the cytokine interleukin-10. IL-10 decreases expression of pro-inflammatory cytokines, such as TNFα and IFNγ, inhibits Th1 cells, and alters macrophage metabolism towards reduced production of ROS and inflammasome activation (Cyktor and Turner, 2011; Ip et al., 2017). These effects dampen inflammatory responses in the context of infection and autoimmunity. Thus, *Salmonella* can suppress pro-inflammatory pathways such as NFκB, and innate immune recognition of *Salmonella* can induce IL10. However, to the best of our knowledge, activation of anti-inflammatory pathways by *Salmonella* secreted effectors has not been previously described.

Here, we leveraged natural diversity among *S. enterica* serovars to reveal a secreted effector (designated SarA, *Salmonella* anti-inflammatory response activator) that promotes IL-10 production and intracellular replication. These effects are mediated by SarA-dependent activation of the transcription factor STAT3. The importance of SarA *in vivo* can be seen in mouse infections, where it promotes virulence at systemic sites, as well as in analysis of non-human clinical isolates that suggests adaptation to bovine hosts.

Results

Natural variation among S. enterica reveals an IL-10 production pathway

In examining responses of lymphoblastoid cell lines (LCLs; Epstein-Barr virus immortalized B cells) to *S.* Typhimurium infection, we noted that *S.* Typhimurium induced robust production of IL-10 protein and transcript (Fig. 1a, b; bacteria and primers in Tables S1 and S2). B cells are *in vivo* targets during *Salmonella* infection (Castro-Eguiluz et al., 2009; Rosales-Reyes et al., 2005). Production of IL-10 in response to *Salmonella* has been observed in macrophages and certain B cell subtypes via TLR4 recognition of LPS (Frankenberger et al., 1995; Neves et al., 2010). This activation is part of immune surveillance and is observed even with dead bacteria or purified LPS. However, the response observed here requires intracellular, living *S.* Typhimurium. Neither heat-killed *S.* Typhimurium nor *S.* Typhimurium unable to invade cells due to mutation of SPI-1 (Δ*prgH*) induced IL-10 (Fig. 1c).

While *S.* Typhimurium induced IL-10, no induction was seen with *S.* Typhi. This presented an opportunity to pair comparative genomics and functional studies to determine the phylogenetic pattern of this activity and identify required genetic elements. We measured IL-10 production in 18 *Salmonella* strains and identified isolates of *Salmonella enterica* serovars Typhimurium, Weltevreden, Newport, and I 4,[5],12:i:- as IL-10-inducers while the remaining strains were unable to induce IL-10 (Fig. 1d). To prevent confounding of our genomic analysis due to strains that had no IL-10 induction secondary to poor SPI-1 mediated entry, we excluded two strains that did not induce SPI-1 mediated pyroptosis (Fig. S1). Comparative genomics of the remaining 16 sequenced strains (Fricke et al., 2011) by pairwise BLASTp of all translated coding sequences (CDS) identified two genes within the Gifsy-1 prophage that were present exclusively in the IL-10 inducing strains. The first gene was *gogB* (STM2584), which as described above is a known anti-inflammatory effector through inhibition of NFκB, while the second gene was *gipA* (STM2599). Due to the known anti-inflammatory properties of GogB, we focused initially on the region around this gene. Genome alignment of *S.* Typhimurium (LT2; IL-10 inducing) and *S.* Heidelberg (SL476; IL-10 non-inducing) revealed a 4869 base pair genetic region, which besides *gogB* includes two other genes (*stm2585* and *pagK2*), all of which were absent from the non-IL-10 inducing strains based on nucleotide BLASTn searches (Fig. 1e, f). Thus, natural variation among Salmonellae revealed a candidate region for the IL-10 phenotype.

Stm2585 (sarA) is required for induction of IL-10 and promotes intracellular replication

Deletion of the 4869bp region resulted in complete loss of *S.* Typhimurium-induced IL-10 (Fig. 2a), while having no effect on bacterial invasion (Fig. S2). To identify the causative gene, we deleted each of the 3 annotated open reading frames in the region. To our surprise, deletion of *gogB* and *pagK2* had no effect on IL-10. In contrast, *stm2585* was necessary for IL-10 induction and was designated *sarA* (*Salmonella anti-inflammatory response activator*) (Fig. 2a). Possibly due to the relatively short length of the open reading frame (546 base pairs / 181 amino acids) and the location within a mosaic prophage region, *stm2585* had not been consistently identified as a coding sequence in other *Salmonella* genomes. This inconsistency was the reason it had not been directly found in our initial gene-based

comparative analysis. Complementation of Δ*sarA* with a plasmid containing *sarA* under its endogenous promoter restored IL-10 induction (Fig. 2b). In addition, introduction of *sarA* to *S. enterica* serovars normally unable to induce IL-10, such as Typhi and Enteritidis, conferred the ability to induce IL-10 (Fig. 2c). *SarA*'s effect was not restricted to LCLs, as Δ*sarA* induced less IL-10 in BJABs (an EBV-negative B-cell lymphoma line) than wild-type *S.* Typhimurium (Fig. 2d). Therefore, *sarA* is necessary and sufficient in the context of *Salmonella* infection to induce IL-10 in B cells.

We next investigated whether *sarA* affected other cellular phenotypes. In the absence of *sarA,* there was reduced intracellular replication by 24 hours post infection, measured as the relative increase in median fluorescence of the GFP+ host cell population (Fig. 2e). In contrast, invasion/early survival (% GFP+ host cells at 3.5 hrs) and pyroptosis, showed no difference with wild-type or Δ*sarA S.* Typhimurium (Fig. S3a, b, c). Within infected LCLs, both wild-type and Δ*sarA S.* Typhimurium were found primarily within LAMP1+ membranes (Fig. S4). Growth of Δ*sarA* was equivalent to wild-type in LB or SPI-2 inducing media, indicating that the intracellular replication difference was due to SarA's interaction with the host (Fig. 2f, g). Notably, exogenous IL-10 was not able to rescue this phenotype, suggesting that reduced intracellular replication is not a consequence of reduced autocrine IL-10 stimulation (Fig. 2h). Thus, SarA's influence is not limited to IL-10 induction but must also involve other host targets that regulate intracellular replication.

SarA is secreted by SPI-1 and SPI-2 T3SS

We determined that SarA was secreted primarily by the SPI-2 T3SS, using β-lactamase (Harmon et al., 2010) fused to the C-terminus of SarA (Fig. 3a, S5a). SarA translocation was greatly attenuated with a nonfunctional SPI-2 (Δ*ssaT*) (Fig. 3b, c), despite equivalent levels of invasion based on CFUs (Fig. 3d). Furthermore, *Salmonella* with mutation of SPI-2 showed a severe decrease in IL-10 induction (Fig. 3e). These results are consistent with published proteomic analysis of *S.* Typhimurium secretomes that identified STM2585 as secreted into the media (Niemann et al., 2011).

Examination of SPI-1's role in SarA translocation is more complex due to the requirement of SPI-1 for entry into non-phagocytic cells (Collazo and Galan, 1997), including LCLs (Alvarez et al., 2017). Therefore, we utilized *S.* Typhi (which does not contain SarA and therefore does not induce IL-10) to trigger macropinocytosis in the LCLs and co-infected with *S.* Typhimurium mutated to have a nonfunctional SPI-1 (Δ*prgH*). The resulting intracellular *S.* Typhimurium Δ*prgH* induced IL-10 nearly as well as wild-type on a per-infected-cell basis (Fig 3e). In contrast, *S.* Typhimurium Δ*ssaT* induced a significantly reduced amount of IL-10, similar to the decrease in SarA translocation as measured by the TEM fusions. Coinfection of *S.* Typhimurium mutated at both SPI-1 and SPI-2 with *S.* Typhi resulted in complete loss of IL-10 induction (Fig. 3e, S5b, c). Therefore, SarA is translocated mainly by the SPI-2 T3SS, with some translocation also by the SPI-1 T3SS.

SarA is required and sufficient for induction of a STAT3 transcriptional program

IL-10 induction is observed at the transcriptional level (Fig. 1b) but is not sufficient to rescue the intracellular replication phenotype (Fig. 2h), which suggested the existence of

other transcriptional targets. RNA-seq was used to compare the transcriptomes of LCLs infected with wild-type vs. Δ*sarA S.* Typhimurium (Fig. 4a). 275 genes were induced at least 2-fold in LCLs infected with wild-type *S.* Typhimurium compared to those infected with Δ*sarA* (Table S3). Gene set enrichment analysis (GSEA) revealed that 3 out of the top 10 enriched pathways involved STAT3 signaling (Fig. 4b; Table S4). This was particularly intriguing because of STAT3's reported role in activating IL-10 transcription in B cells (Ziegler-Heitbrock et al., 2003). In addition to IL-10 (35-fold higher in wild-type; $p=3\times10^{-130}$), other anti-inflammatory STAT3 targets were revealed by the RNA-seq, such as Socs3 (11.6-fold higher; $p=2\times10^{-53}$; blocks IL-6 receptor signaling) (Yasukawa et al., 2003) and Bcl3 (3.2-fold higher; $p=5\times10^{-39}$; suppresses TNF-α expression) (Kuwata et al., 2003).

Consistent with SarA increasing expression of STAT3 targets, we observed SarA-dependent phosphorylation of STAT3 (Fig. 4c). A previous report indicated that *S.* Typhimurium infection results in STAT3 phosphorylation in HeLa and Henle epithelial cells but did not identify the causative effector (Hannemann and Galan, 2017). We confirmed *S.* Typhimurium infection in HeLa and Henle cells results in STAT3 phosphorylation and found that it was greatly diminished with Δ*sarA* (Fig. 4d, e). Similar results were seen in BJABs and THP1 monocytes (Fig. 4f, g). Therefore, SarA is required for STAT3 phosphorylation in a wide range of cell types.

Heterologous expression of SarA in HeLa cells was sufficient for STAT3 phosphorylation (Fig. 4h). Notably, IL-10 protein was not detected from HeLa cells either in response to *S.* Typhimurium infection or *sarA* transfection, suggesting that STAT3 activation is not simply a downstream consequence of IL-10 receptor activation. This distinction is relevant, as STAT3 is also the primary transcription factor downstream of IL-10 receptor signaling (Murray, 2005). In LCLs, expression of SarA was sufficient for both STAT3 phosphorylation and IL-10 production without any *Salmonella* present (Fig. 4i, j).

STAT3 is required for SarA-dependent IL-10 production and effect on intracellular replication

STAT3 inhibition through a small-molecule inhibitor or knockdown via RNAi demonstrated that STAT3 was required for IL-10 induction by *S.* Typhimurium. STAT3 inhibitor VI (Siddiquee et al., 2007), showed a dose-dependent decrease in SarA-dependent IL-10 production (Fig. 5a). RNAi against STAT3 showed even more robust inhibition (Fig. 5b). STAT3 knockdown and infection with wild-type *S.* Typhimurium phenocopied the reduction in intracellular replication demonstrated by Δ*sarA* (Fig. 5c). No further reduction in intracellular replication was observed in combining the STAT3 knockdown with Δ*sarA*—thus it appears the entire reduction in intracellular replication of Δ*sarA* can be attributed to the effect on STAT3.

While *Salmonella* infects B cells *in vivo*, we wanted to determine if similar effects of SarA were observed in other cell types. Specifically, Hannemann et al. (Hannemann et al., 2013) reported that *S.* Typhimurium replication in Henle epithelial cells was partially dependent on STAT3 based on CFU plating. For wild-type *S.* Typhimurium in Henle cells, we observed a four-fold increase in mean fluorescence, similar to the four-fold increase in CFUs previously reported (Hannemann et al., 2013). Similar to our results in LCLs, Δ*sarA* exhibited a modest

reduction (11%) in mean fluorescence of GFP-positive cells compared to wild-type. However, we also detected a decrease in the percentage of GFP-positive cells with Δ*sarA* (20%) (Fig. 5d). Thus, in Henle cells, the reduced burden of *S.* Typhimurium Δ*sarA* could be attributed to decreases in both the percentage of *Salmonella*-infected cells and intracellular replication. These differences could reflect effects on replication and/or susceptibility to host killing that may vary by cell type.

A role for STAT3 in SarA-dependent effects is further supported by physical interaction data. When flag-tagged SarA is transfected into HeLa cells, STAT3 co-immunoprecipitated with flag-tagged SarA but not with the vector only control (Fig 5e). Immunoprecipitation of STAT3 was performed to confirm the interaction. GFP-tagged SarA co-immunoprecipitated with STAT3 while GFP alone demonstrated no interaction (Fig. 5f).

Mutation of SarA caused decreased virulence

We next determined the relevance of SarA during *Salmonella* infection in mice. Δ*sarA* had reduced virulence in intraperitoneal (IP) infections, manifest in both reduced CFUs in spleen and moderately prolonged survival (Fig. 6a, b). Furthermore, competitive index experiments showed reduced fitness of Δ*sarA* even when in the same milieu as wild-type *S.* Typhimurium (Fig. 6c, d). The reduction in competitive index suggests that the effect of SarA on bacterial burden cannot be rescued by the actions of surrounding wild-type bacteria, for example through induction and secretion of IL-10 or other cytokines. This is consistent with the inability of recombinant IL-10 to rescue the intracellular replication phenotype *in vitro*. Therefore, SarA promotes bacterial replication in a cell-autonomous manner during systemic infection.

A competitive chronic oral infection model (CBA/J; (Bogomolnaya et al., 2008)) also demonstrated decreased fitness of Δ*sarA* in the liver and spleen (Fig. 6e). In contrast, no difference was observed in the cecum (Fig. 6e), again supporting the idea of SarA functioning primarily at systemic sites of infection.

The effect of SarA on STAT3 activation was recapitulated *in vivo*. STAT3 phosphorylation was induced by *S.* Typhimurium infection in the spleen at 4 days, but the level of induction was reduced with *ΔsarA* infection (Fig. 6f). While we cannot rule out that the reduced bacterial burden in *ΔsarA*-infected mice contributed to the reductions in p-STAT3, these results are consistent with SarA-dependent activation of STAT3 occurring *in vivo*.

Evidence SarA plays a role in host adaptation

We hypothesized that variation in presence/absence of *sarA* among serovars could be driven by host adaptation. Therefore, we examined national surveillance data on *S. enterica* isolates from CDC's Atlas of Salmonella in the United States, 1968-2011 (CDC, 2013). Three of the four *sarA*-containing serovars (Typhimurium, Newport, and I 4,[5],12:i:-) were included in this atlas. In regards to human infections, there was no significant correlation with presence or absence of the *sarA* gene in the total number of human clinical isolates obtained for serovars from 1968-2011 (Fig. 7a).

This atlas also provides data on non-human isolates, divided into “clinical” isolates, where animals demonstrated signs consistent with salmonellosis, and “non-clinical” isolates, derived from monitoring efforts. While large in scale, the data are not comprehensive. Despite this, known examples of host adaptation are apparent. The serovar displaying the greatest fraction of its isolates from porcine sources (for both clinical (71%) and non-clinical isolates (67%)) was serovar Derby, a known pig-adapted serovar (Hayward et al., 2016), which notably lacks the *sarA* gene. Additionally, for the three serovars showing the greatest percentage of clinical isolates from chickens (Enteritidis, Heidelberg, and Hadar), > 80% of outbreaks in the United States for these serovars were attributed to eggs and poultry (Jackson et al., 2013) and all three lack the *sarA* gene. In comparing the percentage of clinical isolates for each serovar that were obtained from different animal hosts, we observed an association for a greater percentage of bovine clinical isolates for *sarA*-containing serovars (Fig. 7B). No other comparisons of serovars with and without *sarA* within a species were statistically significant (Fig. 7b, c). Thus, natural diversity facilitated the identification of the *sarA* gene but also provided evidence for a role of this effector in infection and adaptation to bovine hosts.

Discussion

Here we identified and characterized SarA as a *Salmonella* effector that alters virulence through induction of a STAT3-dependent anti-inflammatory pathway. This STAT3 activation has cell autonomous effects in promoting intracellular replication, but also non-cell autonomous effects such as production of IL-10. Recently, IL-10 production from lymphocytes was demonstrated to be a significant contributor to systemic *S.* Typhimurium infection in mice (Salazar et al., 2017). IL-10 also has been reported to increase susceptibility to systemic infection during co-infection with *Plasmodium falciparum* (Lokken et al., 2014). Our discovery of *Salmonella* effector-induced IL-10 adds another layer of complexity to the role of this key anti-inflammatory cytokine during infection.

Our work solves a mystery regarding how some *Salmonella* strains are able to activate STAT3. Hannemann et al. suggested that STAT3 activation required the activities of SopB, SopE2, and SopE (Hannemann et al., 2013), and more recently suggested that the lack of STAT3 activation in *S.* Typhi infection was due to an unidentified *S.* Typhi effector blocking STAT3 activation (Hannemann and Galan, 2017). However, we found that SarA is sufficient to confer the ability to activate STAT3 to *S.* Typhi and that mammalian expression of SarA is sufficient to induce STAT3 phosphorylation. This activation likely occurs through physical interactions involving SarA and STAT3, though future structural biology and proteomics analysis will be required to elucidate the molecular details of this activation.

While the genome databases we examined annotated *stm2585* as either “transposase-like protein” (UCSC Genome Browser and EcoGene), “hypothetical protein” (Biocyc and KEGG), or “gifsy-1 prophage protein” (Uniprot), we learned during preparation of this manuscript that *stm2585* had previously been designated *pagJ* (Belden and Miller, 1994; Navarre et al., 2005) and *steE* (Niemann et al., 2011). Despite these annotations, the function and molecular effects of SarA on host cells remained a mystery. Combining comparative

genomics and functional characterization, we provided a molecular role for SarA (induction of IL-10) even prior to our identification of the *sarA* gene.

In addition to identifying SarA, our comparative genomic analysis demonstrated an example of horizontal gene transfer of an anti-inflammatory locus. SarA is contained within the Gifsy-1 prophage, one of three lambda-prophages carrying T3SS effectors in various *S. enterica* serovars (Figueroa-Bossi et al., 2001). This region also encodes GogB and PagK2, which also have roles in virulence. GogB is secreted by SPI-1 and SPI-2 T3SS and is also anti-inflammatory through negatively regulating NFκB (Pilar et al., 2012). PagK2 is secreted in outer membrane vesicles and contributes to intracellular survival in macrophages through an unknown mechanism (Yoon et al., 2011). The proximity of two anti-inflammatory effectors, SarA and GogB, suggests some evolutionary pressure for keeping this anti-inflammatory region of the Gifsy-1 prophage in certain *Salmonella* serovars.

Our work provides evidence for a dichotomy between the pro-inflammatory effects of SPI-1 effectors in the gut early during infection (Hapfelmeier et al., 2004; Keestra et al., 2011; Zhang et al., 2002) and the anti-inflammatory effects of SarA and other SPI-2 effectors such as SpvC (Haneda et al., 2012) and GtgA, GogA, and PipA (Sun et al., 2016) at systemic sites later in infection, when *Salmonella* must evade immunity and promote intracellular growth. SarA activation of STAT3 promotes both goals. Consistent with this model, we observed reduced bacterial burden in systemic sites with both IP and oral infections. Genome-wide studies of *S.* Typhimurium virulence and persistence also support these conclusions. Lawley et al. identified *stm2585* as contributing to long-term systemic infection (Lawley et al., 2006), while Elfenbein et al. found no role in a short-term calf ligated ileal loop model (Elfenbein et al., 2013).

The central importance of STAT3 and IL-10 in both autoimmunity and cancer could mean that there are unintended consequences of STAT3 activation following infection. We speculate that activation of STAT3 by SarA, leading to production of IL-10 by regulatory B cells and other immune cells, could reduce inflammation and risk/severity of autoimmune diseases such as inflammatory bowel disease. Conversely, activation of STAT3 by *Salmonella* could contribute to transformation and intestinal cancer, similar to how *Helicobacter pylori* effector CagA activation of STAT3 promotes gastric cancer (Bronte-Tinkew et al., 2009; Lee et al., 2012). SarA has no significant similarity to CagA and indeed has no known functional domains beyond a predicted transmembrane segment. Future studies will elucidate the role of SarA not only on infection but also explore possible roles in autoimmunity and cancer.

Experimental Procedures

Cells

Lymphoblastoid cell lines (LCLs; Coriell) were grown in RPMI 1640 with 10% fetal bovine serum (FBS), 100 U/ml penicillin (pen), and 100μg/ml streptomycin (strep) (Thermo Fisher). HeLa and Henle cells were grown in DMEM with 10% FBS and pen/strep. BJABs and THP1s were grown in RPMI 1640 with 10% FBS and pen/strep. Cells were grown at 37˚C 5% CO_2. For infections, pen/strep-free media was used.

Salmonella

Salmonella enterica serovar Typhimurium strain 14028s and other strains (Table S1) were grown at 37˚C and 250 RPM in Luria-Bertani (LB) broth (Thermo Fisher). Deletion mutants were made by lambda red recombinase (Datsenko and Wanner, 2000) and verified by PCR (Table S2). For quantification of bacterial invasion and replication, Salmonellae were transformed with pMMB67GFP (Pujol and Bliska, 2003), a plasmid carrying green fluorescent protein under an isopropyl β-D-1-thiogalactopyranoside (IPTG) promoter and maintained with 100μg/mL ampicillin. *SarA* and its endogenous promoter were cloned onto pWSK129 (Wang and Kushner, 1991) to make pWSK129-SarA and maintained with 50μg/mL kanamycin. For competitive index infections, wild-type *S.* Typhimurium contained pWSK129 (kanamycin resistance) and Δ*sarA* contained pWSK29 (ampicillin resistance). For the translocation assay, the β-lactamase (TEM) fragment was amplified from pSR47 (Harmon et al., 2010) using primers TEM1F and TEM1R (Table S2). TEM was cloned into pWSK129-SarA using KpnI and NotI (NEB), creating pWSK129-SarA-TEM. For heat-killed *S.* Typhimurium experiments, *S.* Typhimurium was heat-killed by incubation at 65°C for 1hr.

Cell culture infections

Assaying infection of LCLs and HeLa cells was done as previously described (Ko et al., 2009). Briefly, overnight cultures of *Salmonella* in LB media were subcultured 1:33 and grown for 2 hours and 40 minutes at 37˚C and 250rpm. Cells were infected at multiplicity of infection (MOI) 30 unless otherwise stated in 96 well plates and incubated for 1 hour (LCLs, THP1s, BJABs) or 30 min (HeLas and Henles). Gentamicin was added at 50μg/mL to kill extracellular bacteria and incubated for 1 hour, followed by dilution to 15μg/mL for longer incubation. IPTG was added 75min prior to the desired timepoint. Infection and cell death were measured with a Guava EasyCyte Plus flow cytometer (Millipore). Cell death was measured by 7AAD (7-aminoactinomycin D; Enzo Life Sciences) staining. Intracellular replication was measured as the ratio of GFP intensity at 24 hours over 3 hours. IL-10 protein in the supernatant at 24 hours was measured by human IL-10 ELISA (R&D systems #DY217B). RNA was harvested by RNAprotect and RNeasy kit (Qiagen). cDNA was synthesized with the iScript cDNA synthesis kit (BioRad). Expression was measured by TaqMan probes (Thermo Fisher) on a StepOne qRT-PCR instrument (Thermo Fisher). *S.* Typhi and *S.* Typhimurium co-infection experiments were carried out with Δ*prgH* and Δ*prgH*Δ*ssaT S.* Typhimurium containing the IPTG-inducible GFP plasmid and *S.* Typhi (which does not induce IL-10) without this plasmid. LCLs were plated as described above and infected with *S.* Typhi at MOI10 and Δ*prgH* or Δ*prgH*Δ*ssaT S.* Typhimurium at MOI50 so *S.* Typhi would induce the macropinocytosis necessary for uptake of *S.* Typhimurium deficient in SPI-1 (Δ*prgH*). Δ*ssaT S.* Typhimurium was infected alone at MOI50.

Comparative genomics of Salmonella serovars

To identify loci that could be responsible for IL-10 induction in *S. enterica*, comparative analyses were carried out using protocols and sequence data similar to those described previously (Fricke et al., 2011). Briefly, chromosome sequences from 18 complete or high-quality *S. enterica* draft genomes from isolates with known or presumed IL-10 inducing or

non-inducing capabilities were used for comparative analysis (strains in Table S1). Translated protein-coding sequences (CDS) were compared by BLASTp using the BLAST score ratio (Rasko et al., 2005), which normalizes BLAST scores of matching proteins against the BLAST score of the comparison of each protein against itself. Discarding matches between proteins with a BLAST score of <0.8 all CDS that were both present in all IL-10 inducers and absent from all IL-10 non-inducers were identified with custom Perl scripts. Two CDS (STM2584 (*gogB*) and STM2599 (*gipA*)) were identified as shared by all IL-10 inducers, which was confirmed by chromosome-wide BLASTn searches and visualization in the Artemis Comparison Tool (ACT, http://www.sanger.ac.uk/science/tools/artemis-comparison-tool-act). ACT was used to determine the exact borders of the shared genome fragment around STM2584, which includes STM2585. BLAST score ratio analysis did not initially identify STM2585 as shared by all IL-10 inducers, as this CDS has not been identified in all genomes that were included in the comparative analysis, possibly due to problems of automated programs to correctly call genes within mosaic, heterogeneous genomic regions such as the Gifsy-1 prophage. A BLASTx search was used to check for additional previously unidentified protein-coding sequences in this fragment. The mirror tree was created using Mesquite (Maddison and Maddison, 2008)

Growth curve

S. Typhimurium was inoculated into LB and grown at 37˚C and 250rpm for 15 hours and subcultured 1:100 into LB or LPM (low phosphate, low magnesium media; composition as in (Coombes et al., 2004)). OD600 was measured by spectrophotometer.

Translocation assay

HeLa cells (200,000 cells/well in 6-well plates) were incubated overnight prior to infection at MOI50. After 30 min, gentamicin was added at 50μg/mL. Twenty-two hours post infection, cells were washed twice with PBS, then treated with CCF4-AM (LiveBLAzer™ FRET-B/G Loading Kit with CCF4-AM, Thermo Fisher) for 2 hours at 37C. Staining was assessed by microscopy (Leica SP5) or flow cytometry (BD Canto II).

RNA-seq

LCLs GM19154 and GM19203 (2 million cells/well in 24-well plate) were infected with wild-type or Δ*sarA S.* Typhimurium at MOI50. After 1 hour, gentamicin (50 μg/mL) was added and subsequently diluted to 15 μg/mL after an additional hour. RNA was harvested 24 hours post infection with RNAprotect and RNeasy Plus kit (Qiagen). Samples consisted of three biological replicates from separate experiments. Library preparation, RNA-seq, and analysis were performed by established methods described in Supplemental Experimental Procedures.

Western blotting

Primary antibodies used were: Anti-DDK (FLAG) (Origene, TA50011), Phospho-Y705-STAT3, STAT3, GFP (Cell Signaling Technology, #9145, #9139, and #2956), and β-tubulin E7 (Developmental Studies Hybridoma Bank) and infrared secondary antibodies from LI-

COR (IRDye 800CW Donkey anti-Rabbit IgG and IRDye 680LT Donkey anti-Mouse IgG). Blots were developed and quantified on a LI-COR Odyssey Classic.

RNAi and other cellular treatments

For RNAi, LCLs were plated in Accell siRNA transfection media (GE Dharmacon) and treated with Accell siRNAs (SmartPool; GE Dharmacon) for 72 hours prior to infection with *S.* Typhimurium. LCLs (GM19154) were incubated with STAT3 inhibitor VI, S3I-201 (Santa Cruz Biotechnology) for 1 hour before infection. For recombinant IL-10 treatment, LCLs (GM19154) were treated with 7.5ng/mL recombinant human IL-10 (R&D Systems, #217-IL) after infection with wild-type and Δ*sarA S.* Typhimurium and incubated overnight. Intracellular replication was measured at 24 hours post infection as described above.

Transfections

HeLa cells (2.2×10^5 cells/well in 6-well plates) were plated 24 hours before transfection and transfected with codon-optimized N-terminally FLAG-tagged SarA (GenScript) or N-terminally GFP-tagged SarA or empty vector controls. Transfection was accomplished with Lipofectamine 3000 (ThermoFisher). Cells were harvested 24 hours post transfection and lysed with 75uL of lysis buffer (0.1% Triton X-100, 25mM Tris-HCl, 150mM NaCl, 1mM EDTA, 5% glycerol, Complete Mini Protease Inhibitor Cocktail tablet (Sigma-Aldrich), 10mM NaF, 1mM Na Orthovanadate). LCLs were transfected using the Neon system (Thermo Fisher) at 2.0×10^7 cell/mL in Belzer's UW cold storage solution using one pulse of 1400V for 30ms and recovered in warm complete RPMI. After 48h of recovery, LCLs were infected as described; then 24hpi supernatants were harvested for IL-10 ELISA and cells lysed with 15μL lysis buffer. Lysates were analyzed by western blotting.

Immunoprecipitation

HeLa cells (1.8×10^6 cells/10cm dish 24 hours before transfection) were transfected with pFLAG-SarA as described above. Cells were lysed with 1mL lysis buffer (same as above) and cell lysate was incubated with anti-FLAG magnetic beads (Sigma-Aldrich, #M8823) for 8 hours in 4˚C while rotating, followed by immunoprecipitation using a DynaMag Spin Magnet (Invitrogen, catalog #12320D) and washed 3x with 10 volumes of lysis buffer. Bound protein was eluted using a glycine-HCl pH 3 buffer. For STAT3 immunoprecipitation, HeLa cells were transfected with pGFP-SarA. Cells were lysed with 1mL lysis buffer and lysate was incubated with STAT3 primary antibody (Cell Signaling Technology, #9139) overnight in 4˚C while rotating. Cell lysate and antibody was incubated with Protein G magnetic beads (Cell Signaling Technology #70024S) for 1 hr at 4˚C with rotation, immunoprecipated using a DynaMag Spin Magnet, and washed 3x with lysis buffer. Immunoprecipitated proteins were eluted by boiling in SDS for 10min and analyzed by western blot.

LAMP1 staining

LCLs were centrifuged at 200xg for 5 minutes, washed with PBS, and fixed with 3% paraformaldehyde for 20min at room temperature. Cells were blocked/permeabilized with 0.2% saponin, 5% normal goat serum in PBS for 30 min at room temperature. Cells were

stained with LAMP1 antibody (H4A3; 1:10 dilution; Developmental Studies Hybridoma Bank) in block/permeabilization solution overnight at 4C, followed by anti-mouse Alexa Fluor 555 (1:1000; Thermo Fisher). Images were acquired with an EVOS fluorescence microscope.

Mouse infections

Mouse protocols were approved by Duke University IACUC (Protocol A200-15-07). Oral infection mouse protocols were approved by N.C. State University IACUC. Breeding stock of C57BL/6j mice were obtained from Jackson laboratories and raised in the Duke Breeding Core Facility. Male and female 6-10 week old mice were infected with *S.* Typhimurium intraperitoneally and monitored twice daily for morbidity. For colony-forming unit counts, tissues were weighed and homogenized in PBS using Zirconium Oxide beads (GlenMills, #7305-000031) and a Mini-BeadBeater-24 (Biospec Products). Appropriate dilutions were plated on LB agar + ampicillin (100μg/mL) or kanamycin (50μg/mL) to calculate CFUs per gram. For phosphorylated STAT3, spleens were harvested in Tissue Extraction Reagent 1 (Thermo Fisher, #FNN0071) and homogenized as above. Homogenates were diluted 1:5 and analyzed by western blot. For chronic infections, 8-10 week old CBA/J mice from Jackson Laboratories were given ~10^8 CFU of a 1:1 mixture of WT and Δ*sarA* mutant by gavage. Mice were euthanized at 14 or 24 days post-infection. Cecum, spleen, and liver were harvested, weighed, homogenized, and plated for CFUs.

Statistical methods

P-values were calculated with Graphpad software using unpaired student's t-test or ANOVA with Sidak's multiple post-hoc comparison where appropriate unless otherwise noted.

Supplementary Material

Refer to Web version on PubMed Central for supplementary material.

Acknowledgements:

SLJ was supported by NIH F31AI124544. SLJ, KLG, KJP, and DCK were supported by NIH R01AI118903, a Duke Whitehead Scholarship, Duke MGM startup funds, and a Duke University Core Facility Voucher awarded by the National Center for Advancing Translational Sciences of the NIH under award number UL1TR001117. JRE was supported by start-up funds from NCSU CVM. We thank Brian K. Coombes (McMaster University) and Jacques Ravel (U. of Maryland) for useful early discussion. We thank David Corcoran, the Duke Genomic Analysis and Bioinformatics Shared Resource, and the Duke Sequencing and Genomic Technologies Shared Resource for performing RNAseq and subsequent analysis. We thank the Duke DLAR Breeding Core for maintenance of mouse colony. We thank Sejal Jain for experimental assistance in immunoblotting.

References

Alvarez MI, Glover LC, Luo P, Wang L, Theusch E, Oehlers SH, Walton EM, Tram TTB, Kuang YL, Rotter JI, et al. (2017). Human genetic variation in VAC14 regulates Salmonella invasion and typhoid fever through modulation of cholesterol. Proc Natl Acad Sci U S A 114, E7746–E7755. [PubMed: 28827342]

Belden WJ, and Miller SI (1994). Further characterization of the PhoP regulon: identification of new PhoP-activated virulence loci. Infect Immun 62, 5095–5101. [PubMed: 7927792]

Bogomolnaya LM, Santiviago CA, Yang HJ, Baumler AJ, and Andrews-Polymenis HL (2008). 'Form variation' of the O12 antigen is critical for persistence of Salmonella Typhimurium in the murine intestine. Molecular microbiology 70, 1105–1119. [PubMed: 18826410]

Bronte-Tinkew DM, Terebiznik M, Franco A, Ang M, Ahn D, Mimuro H, Sasakawa C, Ropeleski MJ, Peek RM, Jr., and Jones NL (2009). Helicobacter pylori cytotoxin-associated gene A activates the signal transducer and activator of transcription 3 pathway in vitro and in vivo. Cancer research 69, 632–639. [PubMed: 19147578]

Castro-Eguiluz D, Pelayo R, Rosales-Garcia V, Rosales-Reyes R, Alpuche-Aranda C, and Ortiz-Navarrete V (2009). B cell precursors are targets for Salmonella infection. Microb Pathog 47, 52–56. [PubMed: 19383536]

CDC (2013). National Salmonella Surveillance Annual Report and Appendices, 2013, U.S.D.o.H.a.H. Services, ed. (Atlanta, GA).

Collazo CM, and Galan JE (1997). The invasion-associated type-III protein secretion system in Salmonella - A review. Gene 192, 51–59. [PubMed: 9224874]

Collier-Hyams LS, Zeng H, Sun J, Tomlinson AD, Bao ZQ, Chen H, Madara JL, Orth K, and Neish AS (2002). Cutting edge: Salmonella AvrA effector inhibits the key proinflammatory, anti-apoptotic NF-kappa B pathway. J Immunol 169, 2846–2850. [PubMed: 12218096]

Coombes BK, Brown NF, Valdez Y, Brumell JH, and Finlay BB (2004). Expression and Secretion of Salmonella Pathogenicity Island-2 Virulence Genes in Response to Acidification Exhibit Differential Requirements of a Functional Type III Secretion Apparatus and SsaL. Journal of Biological Chemistry 279, 49804–49815. [PubMed: 15383528]

Cyktor JC, and Turner J (2011). Interleukin-10 and Immunity against Prokaryotic and Eukaryotic Intracellular Pathogens. Infection and Immunity 79, 2964–2973. [PubMed: 21576331]

Datsenko KA, and Wanner BL (2000). One-step inactivation of chromosomal genes in Escherichia coli K-12 using PCR products. Proc Natl Acad Sci U S A 97, 6640–6645. [PubMed: 10829079]

Elfenbein JR, Endicott-Yazdani T, Porwollik S, Bogomolnaya LM, Cheng P, Guo J, Zheng Y, Yang HJ, Talamantes M, Shields C, et al. (2013). Novel determinants of intestinal colonization of Salmonella enterica serotype typhimurium identified in bovine enteric infection. Infect Immun 81, 4311–4320. [PubMed: 24019407]

Figueroa-Bossi N, Uzzau S, Maloriol D, and Bossi L (2001). Variable assortment of prophages provides a transferable repertoire of pathogenic determinants in Salmonella. Molecular microbiology 39, 260–271. [PubMed: 11136448]

Frankenberger M, Pechumer H, and Ziegler-Heitbrock HW (1995). Interleukin-10 is upregulated in LPS tolerance. Journal of Inflammation 45, 56–63. [PubMed: 7583353]

Fricke WF, Mammel MK, McDermott PF, Tartera C, White DG, Leclerc JE, Ravel J, and Cebula TA (2011). Comparative genomics of 28 Salmonella enterica isolates: evidence for CRISPR-mediated adaptive sublineage evolution. Journal of bacteriology 193, 3556–3568. [PubMed: 21602358]

Haneda T, Ishii Y, Shimizu H, Ohshima K, Iida N, Danbara H, and Okada N (2012). Salmonella type III effector SpvC, a phosphothreonine lyase, contributes to reduction in inflammatory response during intestinal phase of infection. Cellular microbiology 14, 485–499. [PubMed: 22188134]

Hannemann S, and Galan JE (2017). Salmonella enterica serovar-specific transcriptional reprogramming of infected cells. PLoS Pathog 13, e1006532. [PubMed: 28742135]

Hannemann S, Gao B, and Galan JE (2013). Salmonella modulation of host cell gene expression promotes its intracellular growth. PLoS Pathog 9, e1003668. [PubMed: 24098123]

Hapfelmeier S, Ehrbar K, Stecher B, Barthel M, Kremer M, and Hardt WD (2004). Role of the Salmonella pathogenicity island 1 effector proteins SipA, SopB, SopE, and SopE2 in Salmonella enterica subspecies 1 serovar Typhimurium colitis in streptomycin-pretreated mice. Infect Immun 72, 795–809. [PubMed: 14742523]

Haraga A, and Miller SI (2003). A Salmonella enterica Serovar Typhimurium Translocated Leucine-Rich Repeat Effector Protein Inhibits NF-κB-Dependent Gene Expression. Infection and Immunity 71, 4052–4058. [PubMed: 12819095]

Harmon DE, Davis AJ, Castillo C, and Mecsas J (2010). Identification and Characterization of Small-Molecule Inhibitors of Yop Translocation in Yersinia pseudotuberculosis. Antimicrobial agents and chemotherapy 54, 3241–3254. [PubMed: 20498321]

Hayward MR, Petrovska L, Jansen VA, and Woodward MJ (2016). Population structure and associated phenotypes of Salmonella enterica serovars Derby and Mbandaka overlap with host range. BMC microbiology 16, 15. [PubMed: 26846255]

Ip WKE, Hoshi N, Shouval DS, Snapper S, and Medzhitov R (2017). Anti-inflammatory effect of IL-10 mediated by metabolic reprogramming of macrophages. Science 356, 513–519. [PubMed: 28473584]

Jackson BR, Griffin PM, Cole D, Walsh KA, and Chai SJ (2013). Outbreak-associated Salmonella enterica serotypes and food Commodities, United States, 1998–2008. Emerg Infect Dis 19, 1239–1244. [PubMed: 23876503]

Jennings E, Thurston TLM, and Holden DW (2017). Salmonella SPI-2 Type III Secretion System Effectors: Molecular Mechanisms And Physiological Consequences. Cell Host Microbe 22, 217–231. [PubMed: 28799907]

Keestra AM, Winter MG, Klein-Douwel D, Xavier MN, Winter SE, Kim A, Tsolis RM, and Baumler AJ (2011). A Salmonella virulence factor activates the NOD1/NOD2 signaling pathway. MBio 2.

Kirk MD, Pires SM, Black RE, Caipo M, Crump JA, Devleesschauwer B, Dopfer D, Fazil A, Fischer-Walker CL, Hald T, et al. (2015). World Health Organization Estimates of the Global and Regional Disease Burden of 22 Foodborne Bacterial, Protozoal, and Viral Diseases, 2010: A Data Synthesis. PLoS Med 12, e1001921. [PubMed: 26633831]

Ko DC, Shukla KP, Fong C, Wasnick M, Brittnacher MJ, Wurfel MM, Holden TD, O'Keefe GE, Van Yserloo B, Akey JM, et al. (2009). A genome-wide in vitro bacterial-infection screen reveals human variation in the host response associated with inflammatory disease. Am J Hum Genet 85, 214–227. [PubMed: 19664744]

Kuwata H, Watanabe Y, Miyoshi H, Yamamoto M, Kaisho T, Takeda K, and Akira S (2003). IL-10-inducible Bcl-3 negatively regulates LPS-induced TNF-α production in macrophages. Blood 102, 4123. [PubMed: 12907458]

Lawley TD, Chan K, Thompson LJ, Kim CC, Govoni GR, and Monack DM (2006). Genome-Wide Screen for Salmonella Genes Required for Long-Term Systemic Infection of the Mouse. PLOS Pathogens 2, e11. [PubMed: 16518469]

Lee KS, Kalantzis A, Jackson CB, O'Connor L, Murata-Kamiya N, Hatakeyama M, Judd LM, Giraud AS, and Menheniott TR (2012). Helicobacter pylori CagA triggers expression of the bactericidal lectin REG3gamma via gastric STAT3 activation. PLoS One 7, e30786. [PubMed: 22312430]

Lokken KL, Mooney JP, Butler BP, Xavier MN, Chau JY, Schaltenberg N, Begum RH, Müller W, Luckhart S, and Tsolis RM (2014). Malaria Parasite Infection Compromises Control of Concurrent Systemic Non-typhoidal Salmonella Infection via IL-10-Mediated Alteration of Myeloid Cell Function. PLOS Pathogens 10, e1004049. [PubMed: 24787713]

Maddison WP, and Maddison DR (2008). Mesquite: A modular system for evolutionary analysis.

Majowicz SE, Musto J, Scallan E, Angulo FJ, Kirk M, O'Brien SJ, Jones TF, Fazil A, Hoekstra RM, and International Collaboration on Enteric Disease 'Burden of Illness, S. (2010). The global burden of nontyphoidal Salmonella gastroenteritis. Clinical infectious diseases : an official publication of the Infectious Diseases Society of America 50, 882–889. [PubMed: 20158401]

Moest TP, and Méresse S (2013). Salmonella T3SSs: successful mission of the secret(ion) agents. In Curr Opin Microbiol, pp. 38–44.

Murray PJ (2005). The primary mechanism of the IL-10-regulated antiinflammatory response is to selectively inhibit transcription. Proc Natl Acad Sci U S A 102, 8686–8691. [PubMed: 15937121]

Navarre WW, Halsey TA, Walthers D, Frye J, McClelland M, Potter JL, Kenney LJ, Gunn JS, Fang FC, and Libby SJ (2005). Co-regulation of Salmonella enterica genes required for virulence and resistance to antimicrobial peptides by SlyA and PhoP/PhoQ. Molecular microbiology 56, 492–508. [PubMed: 15813739]

Neves P, Lampropoulou V, Calderon-Gomez E, Roch T, Stervbo U, Shen P, Kuhl AA, Loddenkemper C, Haury M, Nedospasov SA, et al. (2010). Signaling via the MyD88 adaptor protein in B cells suppresses protective immunity during Salmonella typhimurium infection. Immunity 33, 777–790. [PubMed: 21093317]

Niemann GS, Brown RN, Gustin JK, Stufkens A, Shaikh-Kidwai AS, Li J, McDermott JE, Brewer HM, Schepmoes A, Smith RD, et al. (2011). Discovery of novel secreted virulence factors from

Salmonella enterica serovar Typhimurium by proteomic analysis of culture supernatants. Infect Immun 79, 33–43. [PubMed: 20974834]

Pilar AV, Reid-Yu SA, Cooper CA, Mulder DT, and Coombes BK (2012). GogB is an anti-inflammatory effector that limits tissue damage during Salmonella infection through interaction with human FBXO22 and Skp1. PLoS Pathog 8, e1002773. [PubMed: 22761574]

Pujol C, and Bliska JB (2003). The ability to replicate in macrophages is conserved between Yersinia pestis and Yersinia pseudotuberculosis. Infect Immun 71, 5892–5899. [PubMed: 14500510]

Rasko DA, Myers GSA, and Ravel J (2005). Visualization of comparative genomic analyses by BLAST score ratio. BMC Bioinformatics 6, 2–2. [PubMed: 15634352]

Rosales-Reyes R, Alpuche-Aranda C, Ramirez-Aguilar Mde L, Castro-Eguiluz AD, and Ortiz-Navarrete V (2005). Survival of Salmonella enterica serovar Typhimurium within late endosomal-lysosomal compartments of B lymphocytes is associated with the inability to use the vacuolar alternative major histocompatibility complex class I antigen-processing pathway. Infect Immun 73, 3937–3944. [PubMed: 15972480]

Salazar GA, Peñaloza HF, Pardo-Roa C, Schultz BM, Muñoz-Durango N, Gómez RS, Salazar FJ, Pizarro DP, Riedel CA, González PA, et al. (2017). Interleukin-10 Production by T and B Cells Is a Key Factor to Promote Systemic Salmonella enterica Serovar Typhimurium Infection in Mice. Frontiers in Immunology 8, 889. [PubMed: 28824622]

Siddiquee K, Zhang S, Guida WC, Blaskovich MA, Greedy B, Lawrence HR, Yip MLR, Jove R, McLaughlin MM, Lawrence NJ, et al. (2007). Selective chemical probe inhibitor of Stat3, identified through structure-based virtual screening, induces antitumor activity. P Natl Acad Sci USA 104, 7391–7396.

Stecher B, Robbiani R, Walker AW, Westendorf AM, Barthel M, Kremer M, Chaffron S, Macpherson AJ, Buer J, Parkhill J, et al. (2007). Salmonella enterica serovar typhimurium exploits inflammation to compete with the intestinal microbiota. PLoS Biol 5, 2177–2189. [PubMed: 17760501]

Sun H, Kamanova J, Lara-Tejero M, and Galan JE (2016). A Family of Salmonella Type III Secretion Effector Proteins Selectively Targets the NF-kappaB Signaling Pathway to Preserve Host Homeostasis. PLoS Pathog 12, e1005484. [PubMed: 26933955]

Wang RF, and Kushner SR (1991). Construction of versatile low-copy-number vectors for cloning, sequencing and gene expression in Escherichia coli. Gene 100, 195–199. [PubMed: 2055470]

Winter SE, Thiennimitr P, Winter MG, Butler BP, Huseby DL, Crawford RW, Russell JM, Bevins CL, Adams LG, Tsolis RM, et al. (2010). Gut inflammation provides a respiratory electron acceptor for Salmonella. Nature 467, 426–429. [PubMed: 20864996]

Yasukawa H, Ohishi M, Mori H, Murakami M, Chinen T, Aki D, Hanada T, Takeda K, Akira S, Hoshijima M, et al. (2003). IL-6 induces an anti-inflammatory response in the absence of SOCS3 in macrophages. Nat Immunol 4, 551–556. [PubMed: 12754507]

Yoon H, Ansong C, Adkins JN, and Heffron F (2011). Discovery of Salmonella virulence factors translocated via outer membrane vesicles to murine macrophages. Infect Immun 79, 2182–2192. [PubMed: 21464085]

Zhang S, Santos RL, Tsolis RM, Stender S, Hardt WD, Baumler AJ, and Adams LG (2002). The Salmonella enterica serotype typhimurium effector proteins SipA, SopA, SopB, SopD, and SopE2 act in concert to induce diarrhea in calves. Infect Immun 70, 3843–3855. [PubMed: 12065528]

Ziegler-Heitbrock L, Lotzerich M, Schaefer A, Werner T, Frankenberger M, and Benkhart E (2003). IFN-alpha induces the human IL-10 gene by recruiting both IFN regulatory factor 1 and Stat3. J Immunol 171, 285–290. [PubMed: 12817009]

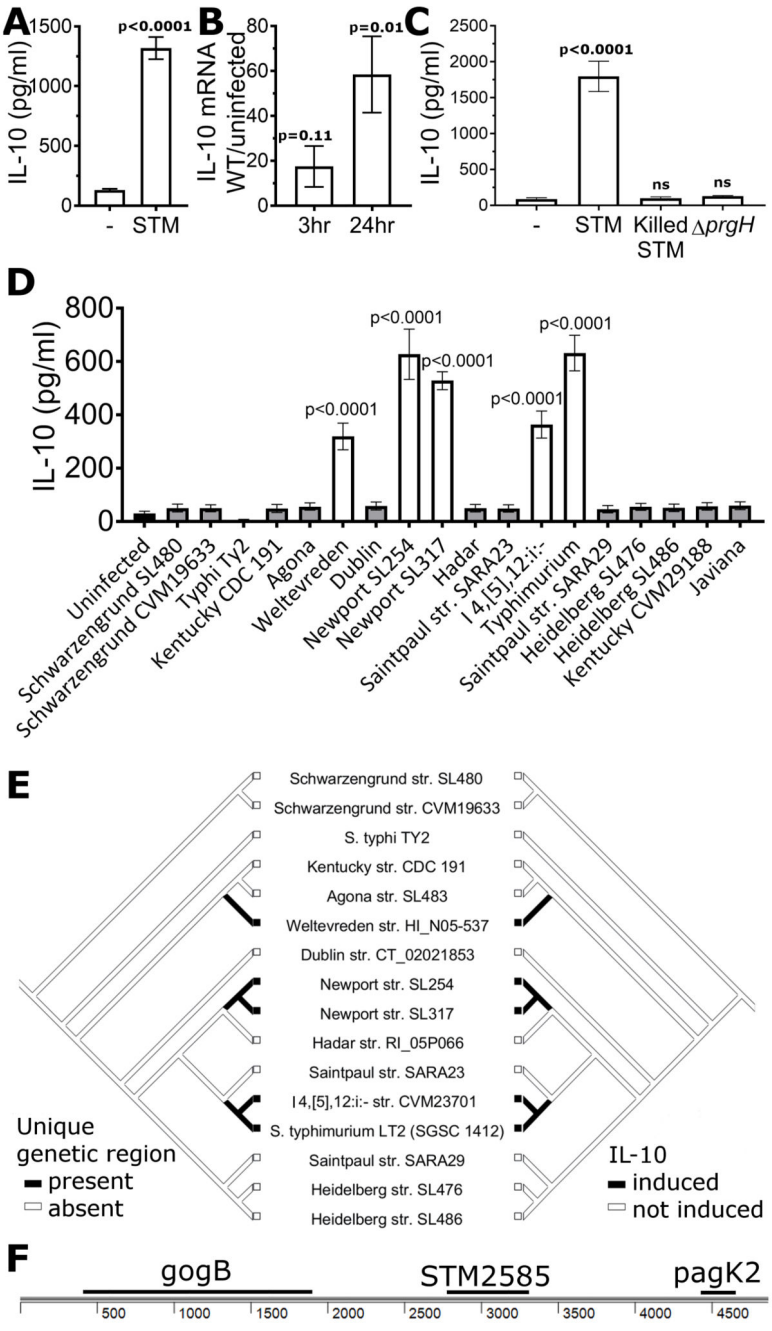

Figure 1: *S.* enterica Typhimurium and other serovars induce IL-10.

a, *S.* Typhimurium induces secretion of IL-10. LCLs (GM19154) were infected with *S.* Typhimurium (STM) at MOI30 and IL-10 in supernatant measured after 24 hrs. **b**, *S.* Typhimurium induces IL-10 at the transcriptional level. IL-10 mRNA levels were measured using Taqman assay of LCLs (GM19154) with and without *S.* Typhimurium infection. For a-b, graphs are from 8-9 biological replicates measured in 3-4 separate experiments. **c**, *S.* Typhimurium induction of IL-10 in LCLs (GM19203) requires living, intracellular *S.* Typhimurium. Heat-killed *S.* Typhimurium or live *S.* Typhimurium unable to invade (Δ*prgH*)

do not induce IL-10 above uninfected levels. 7-10 biological replicates measured in 3 experiments. **d**, *S. enterica* strains exhibit variation in their ability to induce IL-10. LCLs (GM19203) were infected with sequenced *S. enterica* serovars at MOI30, and IL-10 in supernatant measured after 24 hrs. Only serovars Weltevreden, Newport, I 4,[5],12:i:-, and Typhimurium induced IL-10. Data for each strain are from at least 6 biological replicates measured in 3 experiments. Levels of pyroptosis, a SPI-1 dependent process, are shown in Figure S1. **e**, A mirror tree of *S. enterica* strains based on the phylogeny from (Fricke et al., 2011) illustrates the presence of a 4869 bp region only in strains able to induce IL-10. **f**, A 4869bp region containing 3 known protein-coding regions is unique to IL-10-inducing serovars. P-values in Figures 1A and 1B were calculated using unpaired student's t-test and in Figures 1C and 1D using ANOVA with Sidak's multiple comparison post-hoc test; error bars represent SEM.

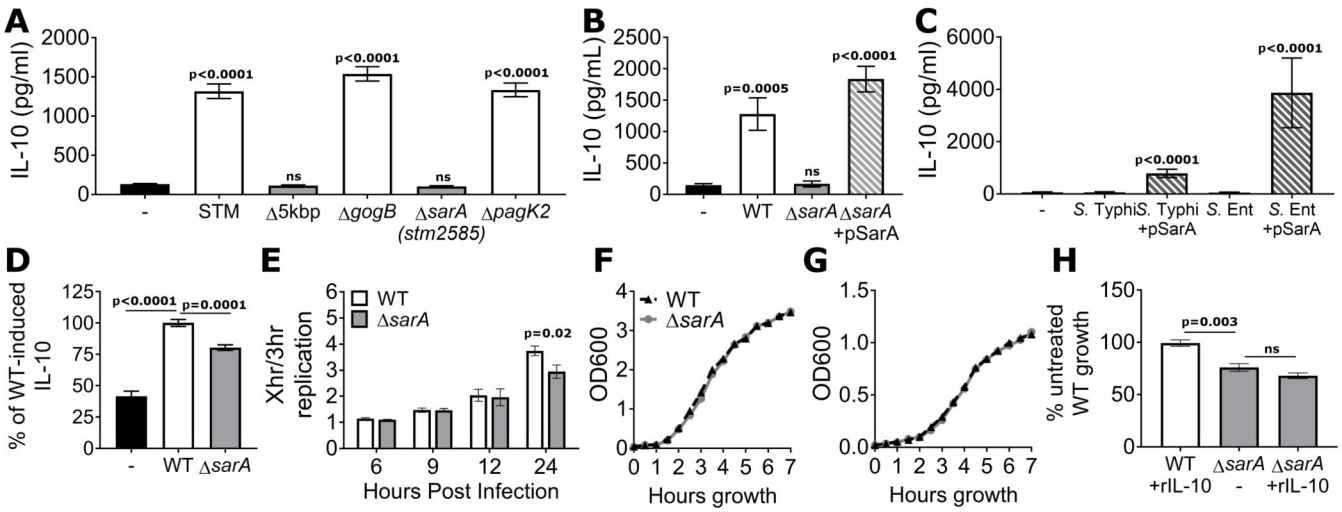

Figure 2. *sarA* (*stm2585*) is required for induction of IL-10 and promotes intracellular replication.

a, *sarA* is necessary to induce IL-10. LCLs (GM19154) were infected with wild-type, the 4869bp deletion mutant (Δ5kbp), or individual deletion mutant *S.* Typhimurium. Δ5kbp and Δ*stm2585* were unable to induce IL-10. **b**, Complementation with pSarA restores IL-10 induction. LCLs were infected with wild-type, Δ*sarA*, or Δ*sarA* containing a plasmid with *sarA* expressed under its endogenous promoter (pSarA). **c**, SarA enables IL-10 induction by serovars naturally unable to induce IL-10. LCLs (GM19203) were infected with *S.* Typhi or *S.* Enteritidis wild-type or containing pSarA. **d**, SarA induces IL-10 in BJABs. Wild-type *S.* Typhimurium induced IL-10 and Δ*sarA* induced significantly less IL-10 in BJABs, controlled per infected cell and presented as percent of wild-type induced IL-10. **e**, Δ*sarA* has an intracellular growth defect. LCLs were infected with GFP-expressing wild-type or Δ*sarA S.* Typhimurium at MOI30 and the bacterial loads were measured by flow cytometry. Intracellular replication was measured as the ratio of increase over the median GFP intensity measured at 3 hours post infection. For a-e, graphs are from 6-9 biological replicates, measured in 3 separate experiments. **f**, SarA does not affect the growth rate of Salmonella alone either in rich media (LB) or **g**, SPI-2-inducing media (LPM). Means of 3 experiments shown. **h**, Decreased growth of Δ*sarA* is not due to its inability to induce IL-10. Addition of recombinant IL-10 did not rescue the intracellular growth defect of Δ*sarA*. P-values in Fig. 2a and 2c are from ANOVA with Sidak's multiple comparison post-hoc test; all other p-values calculated using unpaired student's t test; error bars represent SEM.

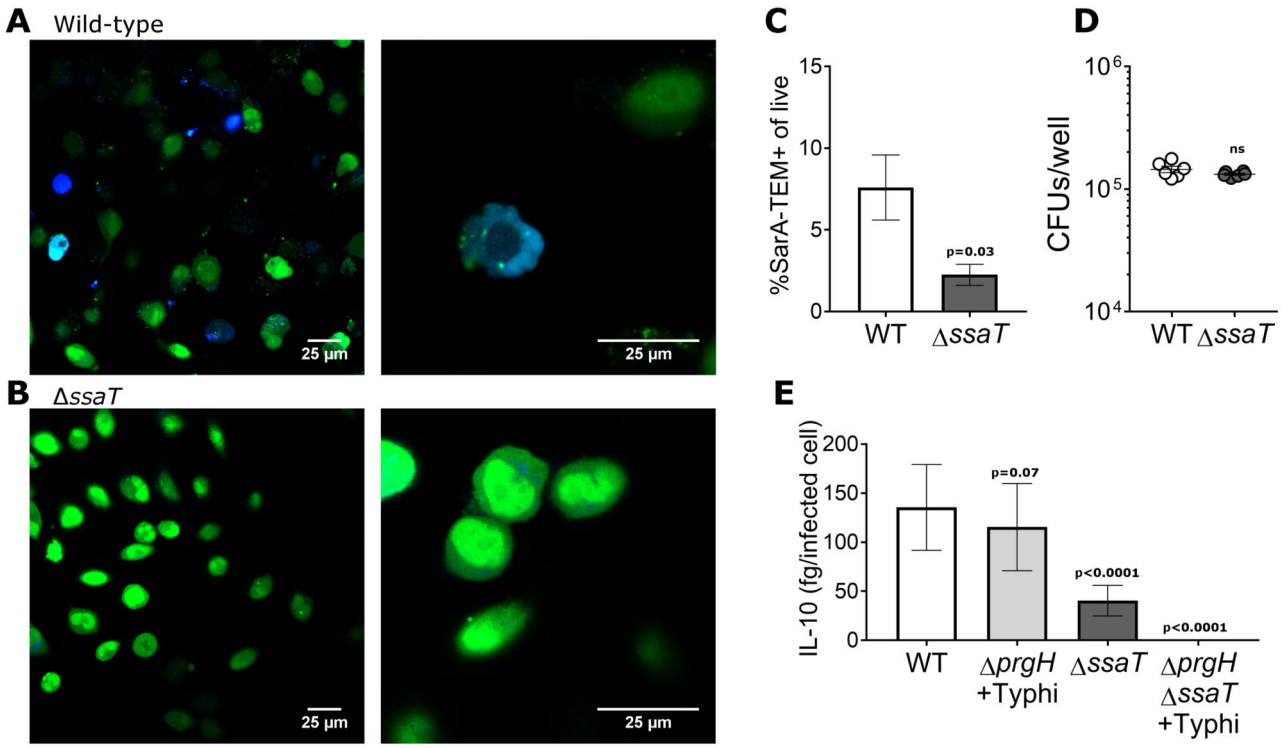

Figure 3. SarA is translocated through both T3SSs of *S.* Typhimurium.

a, SarA-TEM fusions are translocated into host cells. HeLa cells infected with wild-type *S.* Typhimurium showed blue fluorescence, indicating that the SarA-TEM fusion was translocated into the host cell cytoplasm. **b**, SarA translocation occurs primarily through the SPI-2 T3SS. HeLa cells infected with Δ*ssaT S.* Typhimurium showed a reduced number of cells with SarA-TEM activity in the cytosol. **c**, Quantification of SarA-TEM translocation by flow cytometry. 11 replicates over 4 experiments. **d**, Wild-type and Δ*ssaT* invasion are equal. HeLa cells were infected with wild-type and Δ*ssaT* containing pSarA-TEM on a kanamycin resistant plasmid as described, lysed 2 hours post infection and plated to determine invasion. P-values calculated using unpaired student's t test with Welch's correction; error bars represent SEM. **e**, Mutation of both SPI-1 and SPI-2 is required to completely block SarA-induced IL-10 production in LCLs (GM19154). Disruption of the SPI-1 T3SS (Δ*prgH*) resulted in a modest decrease in the amount of IL-10 induced by *S.* Typhimurium that did not reach statistical significance when entry is facilitated by *S.* Typhi. Disruption of the SPI-2 secretion system (Δ*ssaT*) results in a significant decrease in the amount of IL-10 induced by *S.* Typhimurium. Disruption of both the SPI-1 and SPI-2 secretion systems (Δ*prgH*Δ*ssaT*) results in no induction of IL-10 by *S.* Typhimurium. IL-10 represented as femtograms per infected cell; infection measured by GFP+ *S.* Typhimurium in LCLs by flow cytometry. Data are presented as IL-10 per infected cell. IL-10 concentration and invasion percentages are depicted separately in Fig. S5. 6 biological replicates over 3 experiments. P-values calculated using ANOVA with Sidak's multiple comparison post-hoc test, error bars represent SEM.

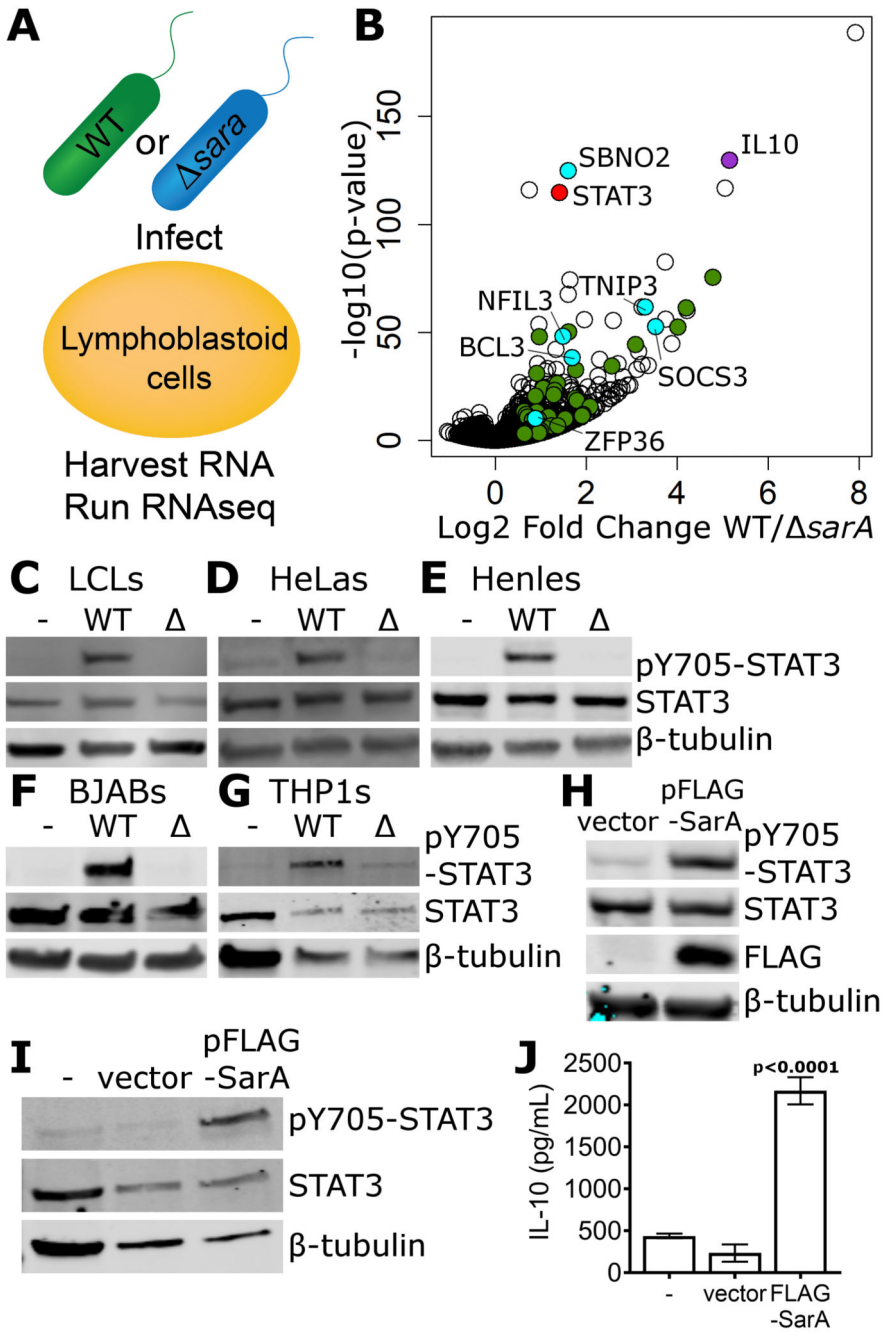

Figure 4. SarA is necessary and sufficient for STAT3 activation.

a, Overview of RNA-seq comparison. LCLs were infected with wild-type or Δ*sarA S.* Typhimurium and harvested at 24 hrs. **b**, Volcano plot of all measured RNA transcripts. IL-10 is labeled and highlighted in purple, STAT3 is labeled and highlighted in red. Known STAT3 targets that show >1.5 fold change with adjusted p-value of <0.05 are highlighted in green, with those known to be involved in mediating an anti-inflammatory response highlighted in cyan and labeled with their gene name. **c, d, e, f, g**, STAT3 phosphorylation in LCLs (**c**), HeLas (**d**), Henles, (**e**) BJABs (**f**), and THP1s (**g**), required SarA. Lysates were

harvested at 24 hrs. **h**, Mammalian SarA expression is sufficient to drive STAT3 phosphorylation. HeLas were transfected with an expression plasmid containing N-terminally FLAG-tagged SarA under a CMV promoter (FLAG-SarA) or with an empty vector control. After 24 hrs, transfected HeLas were harvested and blotted for phosphorylated STAT3, total STAT3, and FLAG. **i**, **j**, Mammalian SarA expression is sufficient to drive STAT3 phosphorylation (**i**) and IL-10 production (**j**) in LCLs at 48 hrs. p-values are from paired t-tests.

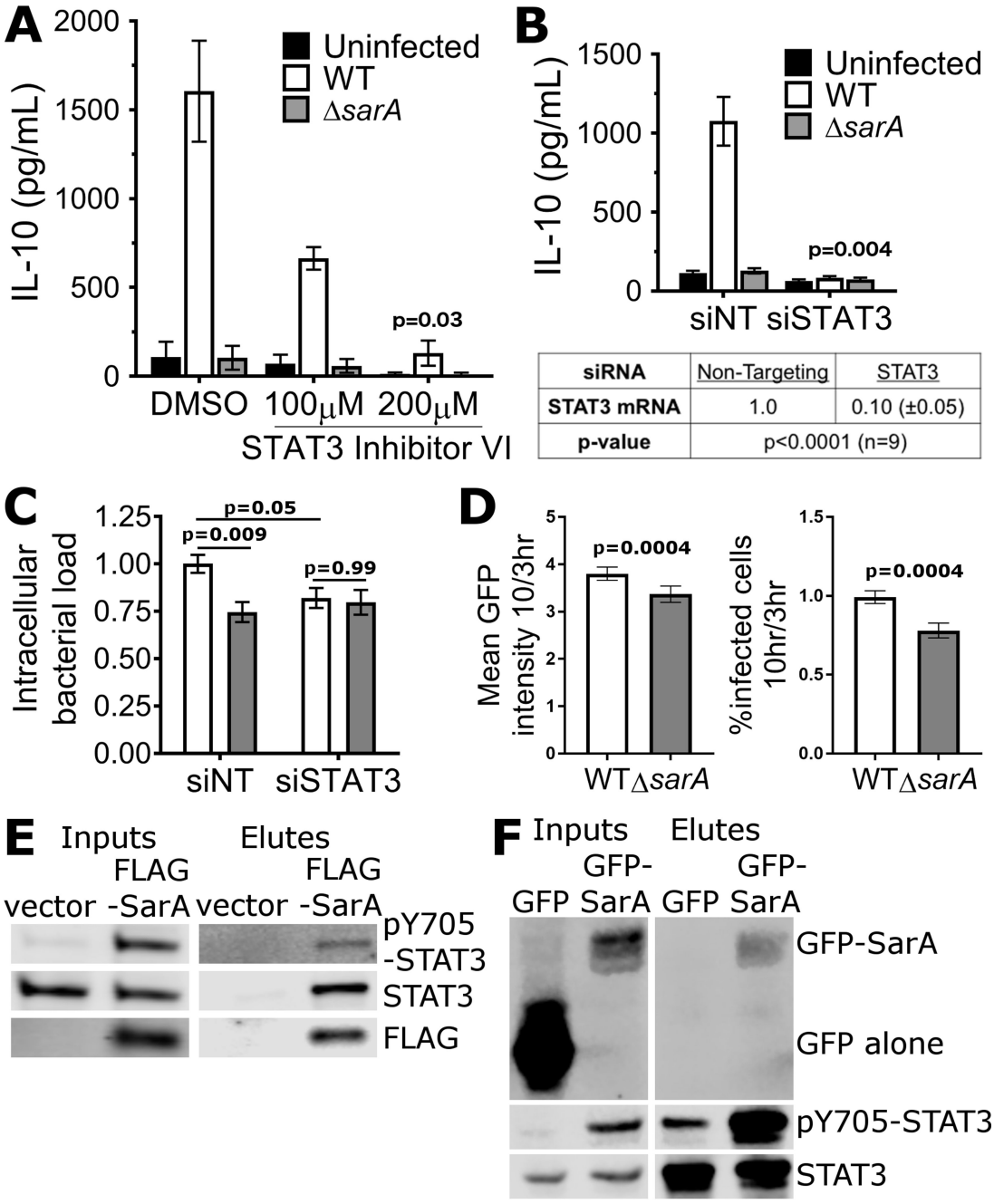

Figure 5. STAT3 activation is required for SarA-induced IL-10 and increased intracellular replication.

a, STAT3 inhibition significantly reduces IL-10 induction by SarA in LCLs (200μM: p = 0.03 by Welch's t-test). DMSO & 100μM are means of three experiments; 200μM is the mean of two experiments. Infection rates were 6.2% wildtype and Δ*sarA* DMSO, 5.5% and 5.8% for wildtype and Δ*sarA* STAT3 inhibitor 100μM; 4% and 4.6% for wildtype and Δ*sarA* STAT3 inhibitor 200μM. No significant differences from wild-type infection with DMSO by ANOVA with Sidak's multiple comparisons post-hoc test. **b**, STAT3 knockdown

significantly blocks IL-10 induction by SarA in LCLs (p = 0.004 by Welch's t-test). 7 wildtype, 5 Δ*sarA* replicates across 4 experiments. qPCR showed ≥90% knockdown of STAT3 mRNA over non-targeting. Infection rates were 4.1% for wild-type with non-targeting, 4.4% for wild-type with STAT3 siRNA, 4.0% for Δ*sarA* with non-targeting, and 4.2% for Δ*sarA* with STAT3 siRNA with no significant differences by ANOVA with Sidak's multiple comparisons post-hoc test. **c**, Knockdown of STAT3 expression significantly reduced *S.* Typhimurium replication and no further reduction was seen with the Δ*sarA* mutant. Median fluorescence was normalized across experiments as fold-change over each experiment's wild-type infected non-targeting. 8 wild-type, 6 Δ*sarA* replicates across 5 experiments. Two-way ANOVA showed significant interaction of siRNA treatment and *Salmonella* genotype (p = 0.04). Displayed p-values are Sidak's multiple comparison post-hoc tests. **a-c**, All error bars on graphs and ±values are SEM. **d**, SarA contributes to intracellular replication and intracellular survival in Henle cells. Henle cells were infected with wild-type or *ΔsarA S.* Typhimurium at MOI5 and the bacterial loads were measured by flow cytometry of GFP expression at 3 and 10 hours post infection. 12 replicates across 4 experiments. P-values calculated by paired t-test. Error bars represent SEM. **e**, STAT3 physically interacts with SarA. HeLa cells were transfected with FLAG-SarA, lysed, and FLAG-SarA immunoprecipitated along with bound proteins. STAT3 was co-immunoprecipitated with FLAG-SarA, but not with vector alone. **f**, SarA physically interacts with STAT3. Hela cells were transfected with pGFP or pGFP-SarA, lysed, incubated overnight with STAT3 antibody, and then STAT3 and bound proteins were immunoprecipitated with protein G magnetic beads. GFP-SarA was co-immunoprecipitated with STAT3 but GFP was not.

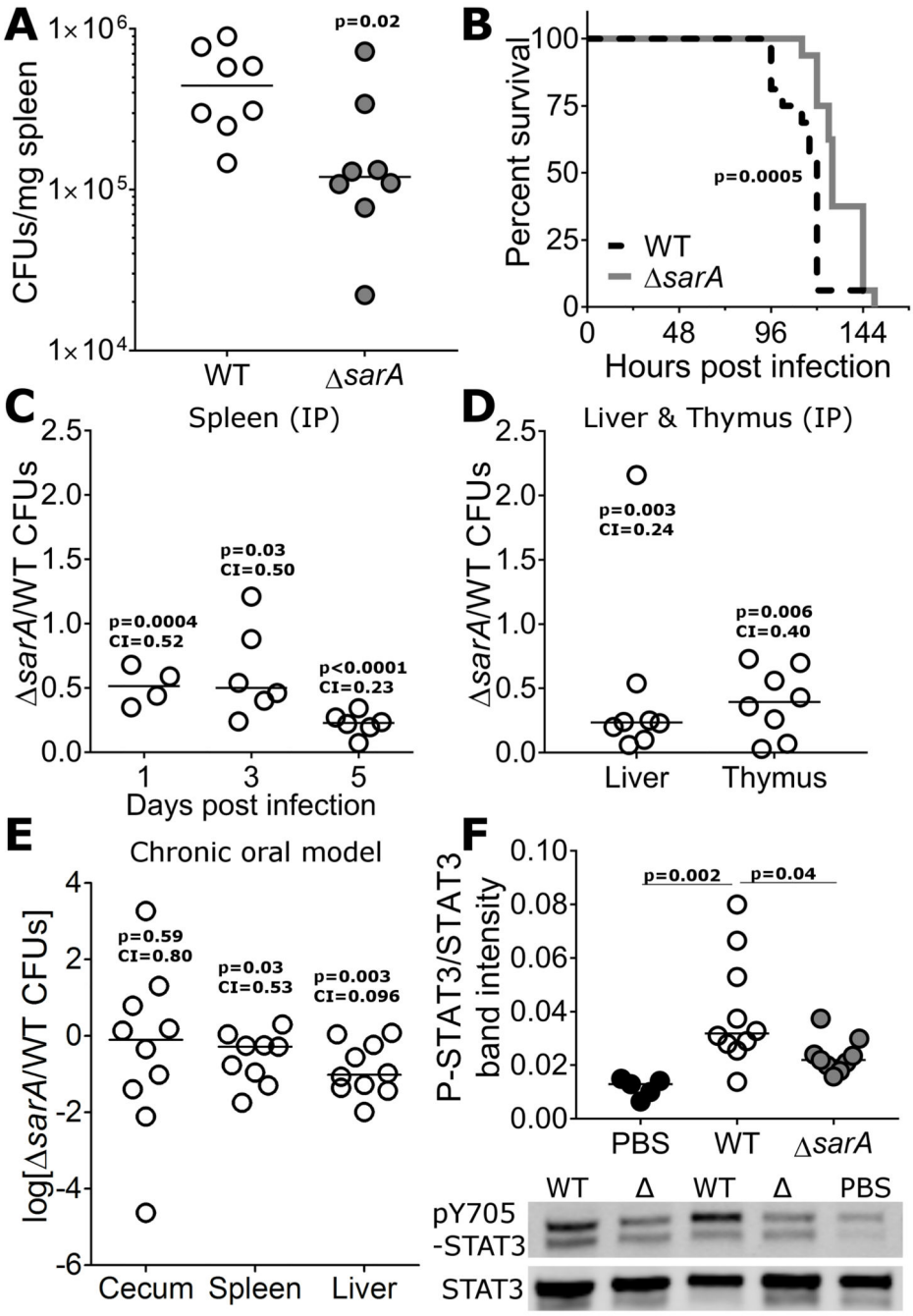

Figure 6. Δ*sarA* shows reduced virulence and reduced p-STAT3 in mice.

a, SarA contributes to bacterial growth in mice. C57BL/6 Mice infected by IP injection with 10^3 wild-type *S.* Typhimurium had significantly higher bacterial loads in the spleen at 5 days than those infected with Δ*sarA.* For all CFU experiments in this figure, line indicates median competitive index, and p-value is from unpaired t-test on log-transformed values. Median competitive index value is provided below p-value. **b**, SarA contributes to virulence in mice. Mice infected as in (a) were monitored until endpoint morbidity was reached, at which point the mice were euthanized. Mice infected with wild-type *S.* Typhimurium succumbed to

infection sooner than mice infected with Δ*sarA*, p = 0.0005 by Log-rank (Mantel-Cox) test. **c, d**, SarA acts cell autonomously to enhance virulence. C57BL/6 mice were infected with ~10^3 CFU of a 1:1 mixture of wild-type *S.* Typhimurium and Δ*sarA* and CFUs were enumerated from spleen (**c**) and thymus (**d**). Wildtype outcompeted Δ*sarA* at each timepoint and the difference increased over time. **e**, SarA has decreased fitness in competitive chronic oral infections. CBA/J mice were orally infected with ~10^8 CFU of a 1:1 mixture of wild-type *S.* Typhimurium and Δ*sarA* mutant by gavage. Data presented are from cecums, livers, and spleens harvested in two separate experiments at either 14 or 24 days post-inoculation. **f**, STAT3 activation is reduced in Δ*sarA.* C57BL/6 mice were infected with ~10^3 wild-type or Δ*sarA S.* Typhimurium. Spleens were harvested 4 days post infection and phosphorylated STAT3 (the upper band, which is the same MW as the primary band in total STAT3) was quantified by western blotting. P-values from Welch's t-test. Data presented are from 3 separate experiments.

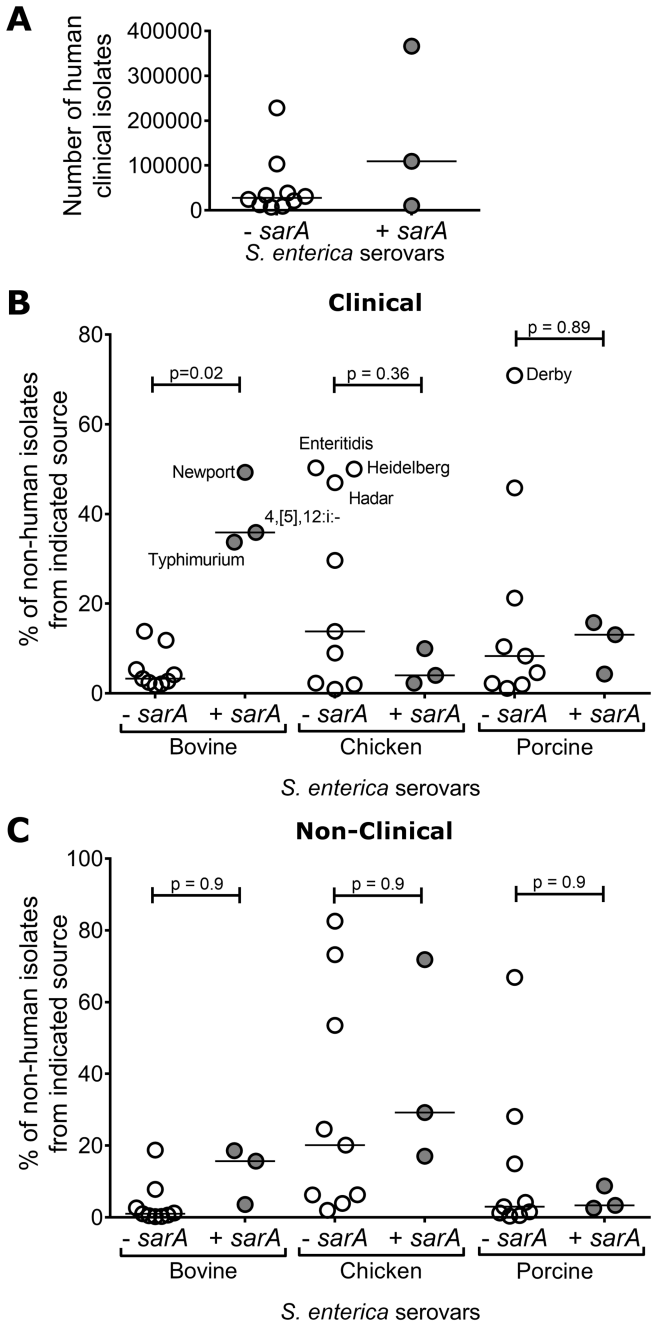

Figure 7. SarA is associated with diversity in serovar host preference.

The CDC's Atlas of *Salmonella* in the United States 1968-2011 (CDC, 2013) was utilized to examine correlation between host species and absence or presence of *sarA* in serovars (assigned in Figure 1). **a**, The number of human clinical isolates of each serovar showed no significant association with the absence or presence of *sarA* ($p = 0.12$ by unpaired t-test, bar indicates median). **b, c**, The percentage of clinical (**b**) and non-clinical (**c**) isolates obtained from bovine, chicken, or porcine sources for each serovar, grouped by absence or presence of *sarA*. Clinical isolates of the serovars containing *sarA* were significantly more likely to be

found in bovine samples compared to clinical isolates for serovars without *sarA* ($p = 0.02$ by ANOVA with Sidak's multiple comparison post-hoc test, bar indicates median). No other pairwise comparisons within hosts were statistically significant.